Fragment mass and kinetic energy distributions for ^{242}Pu(sf), ^{241}Pu(n_{th},f), and ^{242}Pu(γ,f)

H. Thierens, E. Jacobs, P. D'hondt, A. De Clercq, M. Piessens, and D. De Frenne
Nuclear Physics Laboratory, B-9000 Gent, Belgium
(Received 31 October 1983)

Energy correlation measurements were performed for the spontaneous fission of ^{242}Pu, the thermal-neutron-induced fission of ^{241}Pu, and the photofission of ^{242}Pu with 12-, 15-, 20-, and 30-MeV bremsstrahlung. The photofission cross section for ^{242}Pu was determined up to 30 MeV. For ^{242}Pu(sf) the overall kinetic energy distribution is strongly asymmetric and the overall mass distribution has a very high peak yield (9%). Important deviations of the average total kinetic energy release $\langle E_k^* \rangle$ and the average light and heavy fragment masses $\langle m_L^* \rangle$ and $\langle m_H^* \rangle$ from the systematics of Unik *et al.* are also observed for this fissioning system. These effects can be explained in the framework of the static scission point model by the strong preferential formation of a shell-stabilized scission configuration with the neutron number of the heavy and light fragments in the vicinity of the spherical $N=82$ neutron shell and the deformed $N=66$ neutron shell, respectively. A decrease of $\langle E_k^* \rangle$ with the average excitation energy $\langle E_{exc}(E_e) \rangle$, $d\langle E_k^* \rangle / d\langle E_{exc}(E_e) \rangle = -0.30 \pm 0.04$, is observed in the photofission of ^{242}Pu. A study of the energy-mass correlations shows that the mentioned decrease is caused predominantly by a diminution of the shell corrections in the mass region of the spherical $N=82$ neutron shell. A comparison of the mass and kinetic energy distributions obtained in this work for ^{242}Pu, with previously reported results for ^{240}Pu and ^{244}Pu and with scission point model calculations, is also included.

RADIOACTIVITY, FISSION ^{242}Pu(sf).
NUCLEAR REACTIONS, FISSION ^{241}Pu(n_{th},f), ^{242}Pu(γ,f), $E_{\gamma_{max}}=12$, 15, 20, 30 MeV; measured photofission yields, fragment energies E_1, E_2; deduced $\sigma(\gamma,f)$, $N(\mu,E_k)/\langle E_{exc}(E_e) \rangle$.

I. INTRODUCTION

A comparative study of the fragment mass and kinetic energy distributions for spontaneous and induced fission provides information on the coupling of the fission mode to the other degrees of freedom in the transition from the saddle to the scission point. Furthermore, studies of these distributions with changing excitation energy of the compound system reveal how strongly the influence of the shell structures in the nascent fragments on the considered fission characteristics is reduced, increasing the excitation energy.

In previous papers[1,2] we reported our results on the spontaneous fission and photofission of ^{240}Pu and ^{244}Pu. Recently we performed energy correlation measurements for ^{242}Pu(sf), ^{241}Pu(n_{th},f), and the photofission of ^{242}Pu with 12-, 15-, 20-, and 30-MeV bremsstrahlung. The results of this ^{242}Pu study are presented in this paper. Concerning the excitation energy dependence of the fission characteristics for ^{242}Pu, the information available in the literature is very scarce. Dyachenko *et al.*[3] and Allaert *et al.*[4] performed a comparative study of the fissioning systems ^{242}Pu(sf) and ^{241}Pu(n_{th},f). Vorobeva *et al.*[5] studied the variation of the average total kinetic energy with the compound nucleus excitation energy in the fast-neutron-induced fission of ^{241}Pu.

From a fission fragment yield curve measured up to 32 MeV the ^{242}Pu photofission cross section was derived using the photon difference method. This enabled the determination of the average excitation energy of the compound nucleus in the performed photofission experiments.

The results of our study on the excitation energy dependence of the mass and kinetic energy of the fragments in the fission of ^{242}Pu are discussed in the framework of the static scission point model, proposed by Wilkins *et al.*,[6] to show the influence of the shell structures in the nascent fragments on the fission characteristics. A direct comparison with scission point model calculations, performed by Moreau *et al.*,[7] is carried out. Also, a comparison with our previously published ^{240}Pu and ^{244}Pu results is included.

II. EXPERIMENTAL PROCEDURE

For the ^{242}Pu energy correlation measurements nearly the same experimental procedure as in our studies of the fissioning systems ^{240}Pu (Ref. 1) and ^{244}Pu (Ref. 2) was followed. Two Ortec *F* series heavy ion detectors (CF-35-600-60) were mounted symmetrically on both sides of the fission target at an angle of 90° and at a distance of 7 cm to the beam axis. The ^{242}Pu spontaneous fission count rate in this geometry was 180 events per day. The pulse heights of coincident events ($\tau=2$ μs) were recorded in a 4096×4096 channels configuration and stored in blocks of 128 pairs in an INTEL 8085 microprocessor based system. These blocks were transmitted by means of an

RS232 line to a VAX 11/780 system. During the photofission runs an on-line correction of the fission fragment pulses for the γ flash, caused by scattered γ rays and secondary electrons during the linac pulses, was performed. This correction was less than 1% of the pulse height of the fission fragments. The spontaneous fission measurements were performed during shut-down periods of the linac.

Since the spontaneous fission count rate was low and the measurements covered a period of six months, extreme care was taken of the stability of the measuring chains. Therefore each run at a given bremsstrahlung end-point energy or a spontaneous fission measurement was accompanied by a photofission run with 20-MeV bremsstrahlung. The ^{242}Pu photofission runs with 20-MeV bremsstrahlung were calibrated with ^{241}Pu(n_{th},f) using the Schmitt *et al.*[8] calibration procedure and the detector calibration constants of Neiler *et al.*[9] These calibrations were performed with a well-thermalized and collimated neutron beam of the reactor BR1 of the SCK/CEN Mol, Belgium, using completely the same experimental setup and geometry as for the photofission runs. The stability of the system during these calibrations was checked with a ^{252}Cf(sf) source and a precision pulser.

Based on the mass and momentum conservation relations and the detector calibration procedure, the pulse heights of the coincident fission fragments were converted off line in two-dimensional provisional mass (μ) and total kinetic energy (E_k) arrays, $N(\mu,E_k)$, of 120×120 channels. Using an iterative procedure, described by Schmitt *et al.*,[10] two-dimensional preneutron mass (m^*) and total kinetic energy (E_k^*) arrays, $N(m^*,E_k^*)$, of 120×120 channels were deduced from the $N(\mu,E_k)$ arrays.

The neutron emission correction, necessary in this conversion, was based on the neutron emission data of Caïtucoli *et al.*[11] for ^{241}Pu(n_{th},f). Since no information on the neutron emission as a function of the fragment mass is available for ^{242}Pu(sf) and ^{242}Pu(γ,f), the neutron emission curve was multiplied by an appropriate factor in the case of these fissioning systems to obtain the correct average total number of emitted neutrons $\langle\nu_T\rangle$. The $\langle\nu_T\rangle$ values for ^{242}Pu(sf), 2.15±0.02, and for ^{241}Pu(n_{th},f), 2.93±0.01, were adopted from Boldeman[12] and Caïtucoli *et al.*,[11] respectively. Up to now data on the $\langle\nu_T\rangle$ values for the photofission of ^{242}Pu were not reported. Consequently the average total number of neutrons, emitted in the photofission of ^{242}Pu, was calculated based on the linear dependence of $\langle\nu_T\rangle$ on the excitation energy, deduced by Condé *et al.*[13] from fast neutron induced fission data on ^{241}Pu. These authors reported for the slope $d\langle\nu_T\rangle/dE_{exc}$ a value 0.146/MeV. Differences in the $\langle Q\rangle$ values between photofission and neutron induced fission, owing to differences in the mass distributions, were also taken into account in the calculation of the $\langle\nu_T\rangle$ values in photofission. The $\langle Q\rangle$ values were calculated as outlined in a previous paper.[2] A correction of the $\langle\nu_T\rangle$ values for photofission, owing to the systematic difference between the average kinetic energy release in photofission and neutron induced fission, observed in this work (Sec. III B), was also carried out. The resulting total correction of the $\langle\nu_T\rangle$ values was very small ($\simeq$0.06 neutrons).

For the determination of the photofission cross section of ^{242}Pu up to 30 MeV, a fission fragment yield curve was measured for bremsstrahlung end-point energies between 10 and 32 MeV. The same experimental setup as for the ^{240}Pu and ^{244}Pu (Refs. 1 and 2) yield measurements was used. The measuring bin width was 500 keV. The behavior of the yield curve from the threshold up to 7.5 MeV was derived from the cross section data of Rabotnov *et al.*[14] In the remaining energy region from 8 up to 9.5 MeV an interpolation between the data of Rabotnov *et al.*[14] and our results was performed. The cross section was derived from the yield curve using the method of Crawford *et al.*[15] with effective decorrelation of the errors of the photon difference data. To obtain the absolute values of the cross section the ^{242}Pu target was replaced by a ^{235}U target with the same dimensions, and a normalization relative to the photofission of ^{235}U with 12- and 18-MeV bremsstrahlung was performed. For this normalization the cross section data of Caldwell *et al.*[16] were used.

The ^{242}Pu target consisted of a 90 μg/cm^2 PuF_3 layer on a 30 μg/cm^2 polyimide backing with 10 μg/cm^2 gold. This target was prepared by evaporation. The isotopic enrichment of the used material was 99.74%. The ^{241}Pu calibration target with a thickness of 41 μg/cm^2 was prepared by electrospraying of plutonium acetate on an identical backing as the ^{242}Pu target. The isotopic enrichment of the ^{241}Pu material was 91%. The diameter of the active layer was 25 mm in both cases. The targets were prepared by the sample preparation group of the Central Bureau for Nuclear Measurements Euratom-Geel (Belgium).

III. RESULTS AND DISCUSSION

A. Photofission cross section and average excitation energies

The cross section for the photofission of ^{242}Pu up to 30 MeV obtained from our experiments is presented in Fig. 1. The calculation of the error bars was based on the statistical uncertainties on the measured yields. An estimation of the absolute uncertainties on the cross section values can be obtained by taking into account a systematic contribution of 10%, owing to the uncertainties on the ^{235}U photo-

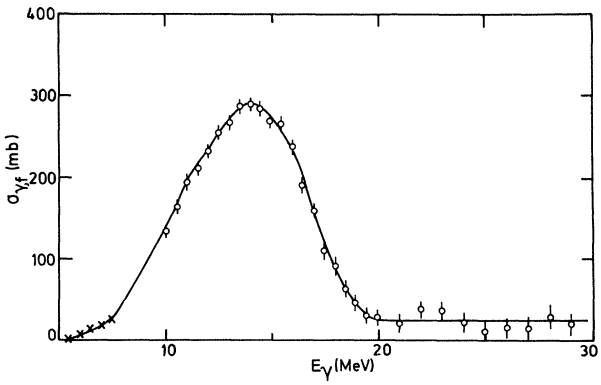

FIG. 1. Photofission cross section of ^{242}Pu, including second and multiple chance fission.

fission cross section data of Caldwell *et al.*[16] and the thickness of the targets. The crosses in Fig. 1 represent the photofission cross section up to 7.5 MeV, adopted from Rabotnov *et al.*[14]

The ^{242}Pu photofission cross section shows the typical giant resonance structure with a maximum around 14 MeV as usually observed for actinide nuclei. The maximum value and the full width at half maximum height amount to 290 mb and 7.0 MeV, respectively. For the integrated cross section up to 20 MeV a value 2.1 ± 0.1 MeV b was found. In the photon energy range above the giant resonance from 20 to 30 MeV the cross section is low (20 mb) and constant within the error bars as observed in our ^{240}Pu and ^{244}Pu photofission studies.

From the ratio of the fission yields in the photofission of ^{235}U and ^{242}Pu with 12-MeV bremsstrahlung a value of 1.02 ± 0.17 was deduced for the neutron emission width to fission width ratio Γ_n/Γ_f for ^{242}Pu. This calculation was based on the photonuclear study of Caldwell *et al.*,[16] who showed that for actinides the total photon absorption cross section is nearly independent of the compound nucleus and that Γ_n/Γ_f is nearly constant above 9 MeV. A Γ_n/Γ_f value of 1.4 for ^{235}U was adopted from the same authors. From (t,pf) experiments at an excitation energy of 2 MeV above the neutron binding energy, Cramer and Britt[17] deduced $\Gamma_n/\Gamma_f=1.3$ for ^{242}Pu, while Vandenbosch and Huizenga[18] reported 0.74 for the Γ_n/Γ_f value derived from the 2 MeV neutron induced fission cross section. In view of the method used for the determination of Γ_n/Γ_f, the literature values are in reasonable agreement with our result.

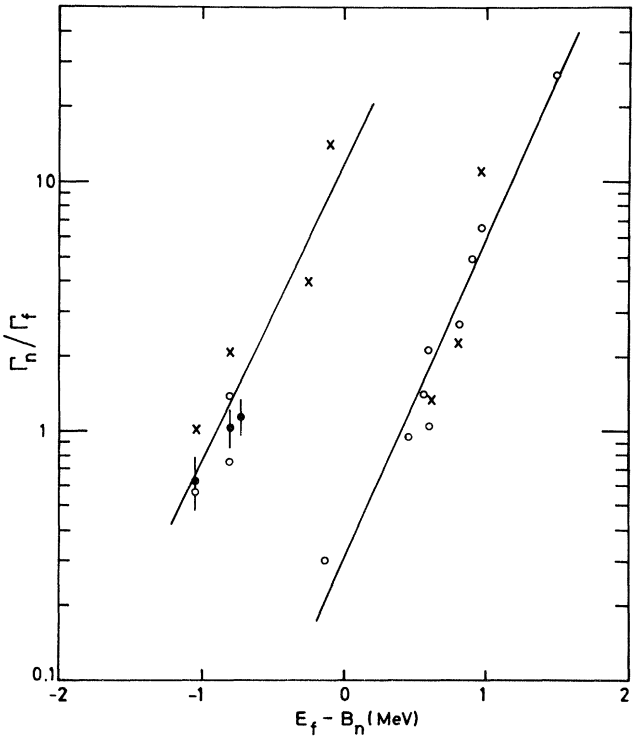

FIG. 2. Behavior of Γ_n/Γ_f as a function of the difference between the fission barrier height and neutron binding energy E_f-B_n. The Γ_n/Γ_f values obtained by Caldwell *et al.* (Ref. 16) from photonuclear measurements are indicated by the crosses. The open circles represent the Γ_n/Γ_f values deduced by Vandenbosch and Huizenga (Ref. 18) from the 2 MeV neutron induced fission cross section; the closed circles are our results for the plutonium isotopes. The full lines are least squares fits to the results for even-even (left) and even-odd (right) fissioning nuclei.

The exponential decrease of Γ_n/Γ_f with Z^2/A, deduced by Caldwell *et al.*[16] from photonuclear data on ^{232}Th and different uranium isotopes, yields an expectation value $\Gamma_n/\Gamma_f=0.52$ for ^{242}Pu, significantly lower than the experimental value, 1.02 ± 0.17, obtained in our work. An extrapolation of the systematic behavior, deduced by Caldwell *et al.*,[16] outside the Z^2/A range considered by these authors is unreliable as already mentioned in our ^{240}Pu paper.[1] In Fig. 2 the Γ_n/Γ_f values, reported by Caldwell *et al.*[16] and those deduced from the 2 MeV neutron induced fission cross section,[18] together with our results for the plutonium isotopes[1,2] are plotted against the difference between the experimental fission barrier heights and the neutron binding energies, E_f-B_n. The values for the fission barrier height were adopted from Britt[19] and the neutron binding energies from the tables of Wapstra and Bos.[20] The full lines are least squares fits to the data. The fits to the results for even-even and even-odd fissioning nuclei are shown on the left- and the right-hand side, respectively. Figure 2 shows that Γ_n/Γ_f depends exponentially on E_f-B_n. As outlined by Vandenbosch and Huizenga,[18] this behavior can be expected in a simple model with a constant temperature level density expression for the nuclear level density. These authors show that the displacement between the results for even-even and even-odd fissioning systems is caused by the influence of the pairing gap on the level densities. This displacement is equal to $\Delta_f+\Delta_n$, with Δ_f the pairing gap at the saddle point, and Δ_n the pairing gap at the equilibrium deformation appropriate to neutron emission. From the least squares fits shown in Fig. 2 we can deduce $\Delta_f+\Delta_n\simeq1.2$ MeV, a reasonable value in comparison with $\Delta_n\simeq0.6$ MeV deduced from the even-odd fluctuations in the ground state mass behavior in this mass region. We can conclude here that an exponential decrease of Γ_n/Γ_f with Z^2/A, as proposed by Caldwell *et al.*,[16] is not compatible with our results and that the values of the fission barrier height and the neutron binding energy have to be taken into account in a systematic study of Γ_n/Γ_f.

Starting from the determined differential photofission cross section the average excitation energy of the fissioning ^{242}Pu nucleus, irradiated with bremsstrahlung with an end-point energy E_e, $\langle E_{\rm exc}(E_e)\rangle$, was calculated using the Schiff[21] form for the bremsstrahlung spectrum. As $\langle E_{\rm exc}(E_e)\rangle$ values for irradiations with 12-, 15-, 20-, and 30-MeV bremsstrahlung, we obtained 9.4, 11.1, 12.5, and 13.2 MeV, respectively. These values are nearly the same as those calculated for the photofission of ^{240}Pu and ^{244}Pu.

A direct calculation of the second chance fission contribution in the performed ^{242}Pu photofission experiments is impossible, since information on the first and second chance photofission cross section for ^{242}Pu is not available. A crude estimation of this contribution in the ^{242}Pu experiments with 12-, 15-, and 20-MeV bremsstrahlung

TABLE I. Parameters of the overall kinetic energy and mass distributions for ^{242}Pu(sf), ^{241}Pu(n_{th},f), and ^{242}Pu(γ,f).

	^{242}Pu(sf)	^{241}Pu(n_{th},f)	^{242}Pu(γ,f) E_e=12 MeV	E_e=15 MeV	E_e=20 MeV	E_e=30 MeV
Number of fission events	14 610	43 112	23 125	88 725	501 566	177 966
$\langle E_k \rangle$ MeV	180.16± 0.20	176.93±0.06	174.34±0.12	173.59±0.15	173.07±0.10	172.86±0.17
$\langle E_k^* \rangle$ MeV	181.69± 0.20	179.00±0.06	176.85±0.12	176.25±0.15	175.88±0.10	175.72±0.17
σ_{E_k} (MeV)	11.24± 0.18	12.04±0.04	11.63±0.13	11.70±0.09	11.80±0.08	11.91±0.06
$\langle \mu_L \rangle$ (u)	104.89± 0.10	102.98±0.03	102.48±0.07	102.50±0.07	102.61±0.06	102.78±0.07
$\langle \mu_H \rangle$ (u)	137.11± 0.10	139.02±0.03	139.52±0.07	139.50±0.07	139.39±0.06	139.22±0.07
$\sigma_{\mu_L}=\sigma_{\mu_H}$ (u)	5.27± 0.08	6.79±0.02	6.84±0.06	7.09±0.05	7.24±0.06	7.36±0.06
$\langle m_L^* \rangle$ (u)	104.62± 0.10	102.47±0.03	101.93±0.07	101.90±0.07	101.98±0.06	102.13±0.07
$\langle m_H^* \rangle$ (u)	137.38± 0.10	139.53±0.03	140.07±0.07	140.10±0.07	140.02±0.06	139.87±0.07
P/V	500 ±180	33 ±3	50 ±7	25.3 ±1.7	15.2 ±0.4	11.1 ±0.4
$\langle E_{exc} \rangle$ (MeV)	0	6.3	9.4	11.1	12.5	13.2

was deduced from the determined total photofission cross section by adopting the dependence of the first chance photofission cross section to the total photofission cross section ratio on the photon energy for ^{236}U from Caldwell *et al.*[16] In this way values of 0%, 8%, and 18% were obtained. These estimations are reasonable in view of the Γ_n/Γ_f values for ^{235}U,[17] ^{236}U,[17] ^{241}Pu,[19] and our Γ_n/Γ_f result for ^{242}Pu. The first chance to the total photofission cross section ratio at photon energies above the (γ,nf) threshold deduced from these Γ_n/Γ_f values are 0.54 and 0.65 for ^{236}U and ^{242}Pu, respectively. This estimation value for ^{236}U is in good agreement with the experimentally determined value of 0.50, obtained by Caldwell *et al.*[16]

B. Kinetic energy

In Table I the main characteristics of the fragment kinetic energy and mass distributions obtained in the present work are summarized. The average values of the total postneutron and preneutron kinetic energy and the rms width of the kinetic energy distributions are denoted by $\langle E_k \rangle$, $\langle E_k^* \rangle$, and σ_{E_k}, respectively. The uncertainties on the values, given in Table I, are the rms deviations for at least seven experimental runs. For a comparison of the $\langle E_k^* \rangle$ values obtained in the present work for ^{242}Pu with the results of other authors and previously published data on ^{240}Pu and ^{244}Pu, an additional systematic contribution of 300 keV has to be added to the uncertainties given in Table I. This systematic contribution is owing to the experimental uncertainty on the energy loss of the fission fragments in the ^{241}Pu and ^{242}Pu targets which were used.

Comparative energy correlation measurements for ^{242}Pu(sf) and ^{241}Pu(n_{th},f) were already performed by Dyachenko *et al.*[3] and Allaert *et al.*[4] The $\langle E_k^* \rangle$ values as well as the difference between ^{242}Pu(sf) and ^{241}Pu(n_{th},f), 2.7±0.6 MeV, obtained in our work, are in perfect agreement with the results of the latter authors. They reported for the $\langle E_k^* \rangle$ values for ^{242}Pu(sf) and ^{241}Pu(n_{th},f) 181.78±0.09 MeV and 178.97±0.07 MeV, respectively. Taking into account the mentioned systematic errors, our result for ^{242}Pu(sf) is also in agreement with the value of Dyachenko *et al.*,[3] 182.22±0.13 MeV. For ^{241}Pu(n_{th},f), however, these authors found a slightly higher value, 179.62±0.03 MeV.

A direct comparison of the overall total kinetic energy distributions for ^{242}Pu(sf) and ^{241}Pu(n_{th},f) is presented in Fig. 3. From this figure it is clear that, where the distribution for thermal-neutron-induced fission shows a Gaussian shape, a significant deviation from a Gaussian is present for spontaneous fission. The decomposition of the overall kinetic energy distribution for ^{242}Pu(sf) and ^{241}Pu(n_{th},f) into the partial distributions for the mass splits with the heavy fragments in the mass region 130—135 and for the remaining mass splits, presented in Fig. 4, shows that the different behavior for spontaneous and thermal-neutron-induced fission can be attributed to mass splits with the heavy fragments in the 130—135 mass region. This was also observed in our study of ^{240}Pu.

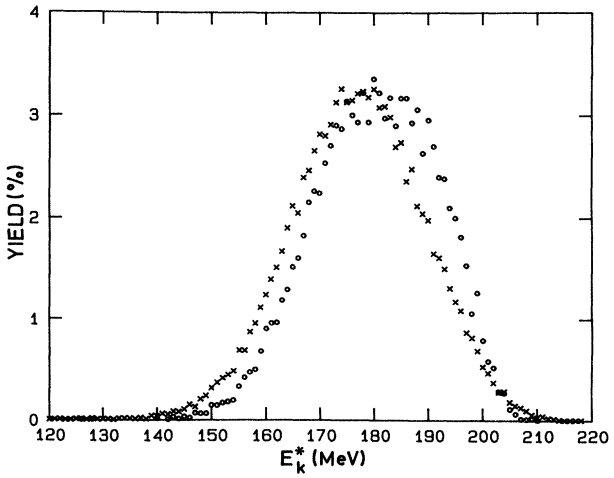

FIG. 3. Comparison of the overall total kinetic energy distributions for ^{242}Pu(sf) (circles) and ^{241}Pu(n_{th},f) (crosses).

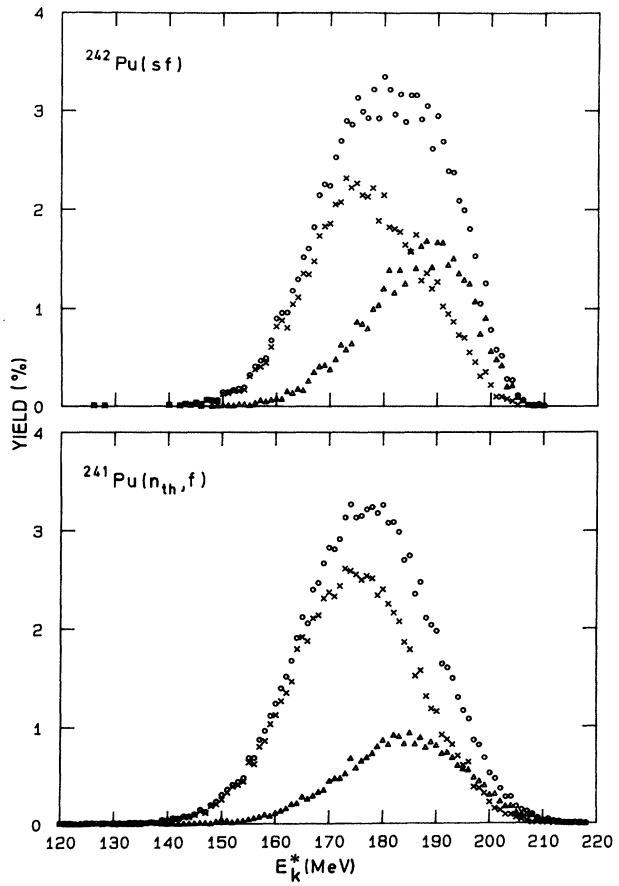

FIG. 4. Decomposition of the overall total kinetic energy distributions (circles) for ^{242}Pu(sf) and ^{241}Pu(n_{th},f) into the partial distributions for the mass splits with the heavy fragments in the mass region 130–135 (triangles) and outside this region (crosses).

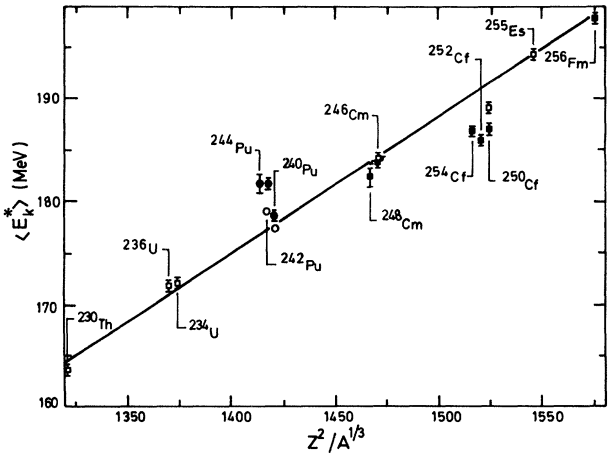

FIG. 5. Correlation between the experimental $\langle E_k^* \rangle$ values for spontaneous (closed symbols) and thermal-neutron-induced (open symbols) fission and the Coulomb repulsion parameter $Z^2/A^{1/3}$. The results reported by Unik *et al.* (Ref. 22) are indicated by the squares. The circles refer to the values for the plutonium isotopes obtained in our work.

The value -0.49 of the dissymmetry coefficient μ_3/σ^3 of the distribution corresponding to the mass region 130–135 for ^{242}Pu(sf) is reduced to -0.26 in ^{241}Pu(n_{th},f). The asymmetry of the partial distributions for the other mass splits is much smaller and remains practically unchanged: $\mu_3/\sigma^3 = -0.05$ for ^{242}Pu(sf) and $\mu_3/\sigma^3 = -0.08$ for ^{241}Pu(n_{th},f). The observed asymmetry for spontaneous fission with a high yield for high kinetic energy events in the mass region 130–135 can be understood in the static scission point model[6,7] by the strong influence of the spherical $N=82$ neutron shell in the heavy fragments. For the fissioning system ^{242}Pu this effect is enhanced by the presence of the deformed $N=66$ neutron shell in the light fragments. In the framework of this model the asymmetry is caused by the preferential formation of the shell-stabilized configuration with low total deformation ($\epsilon_2^{(1)}+\epsilon_2^{(2)} \simeq 0.8$), compared to a secondary configuration with larger total deformation ($\epsilon_2^{(1)}+\epsilon_2^{(2)} \simeq 1.4$), favored by the liquid drop behavior. Owing to the diminution of the shell correction terms in the potential energy at higher intrinsic temperatures, the importance of the shell-stabilized configuration is decreased in induced fission compared to spontaneous fission. This effect is responsible for the disappearance of the asymmetry in the overall kinetic energy distribution for ^{241}Pu(n_{th},f).

Unik *et al.*[22] have studied the correlation between the experimental values of the average total kinetic energy release $\langle E_k^* \rangle$ for spontaneous and thermal-neutron-induced fission and the Coulomb repulsion parameter $Z^2/A^{1/3}$. In Fig. 5 the $\langle E_k^* \rangle$ values for spontaneous and thermal neutron induced fission of the plutonium isotopes, obtained in our work, are compared to the systematics of Unik *et al.*[22] The higher kinetic energies for the spontaneous fission of the plutonium isotopes, and especially for ^{242}Pu(4.4 MeV) and ^{244}Pu(5.0 MeV), are mainly owing to the strong influence of the spherical $N=82$ neutron shell.

A linear fit to the ^{242}Pu photofission data using a weighted least squares procedure yields a value -0.30 ± 0.04 for the slope $d\langle E_k^* \rangle / d\langle E_{exc}(E_e) \rangle$. Taking into account the error bars, this value is not significantly

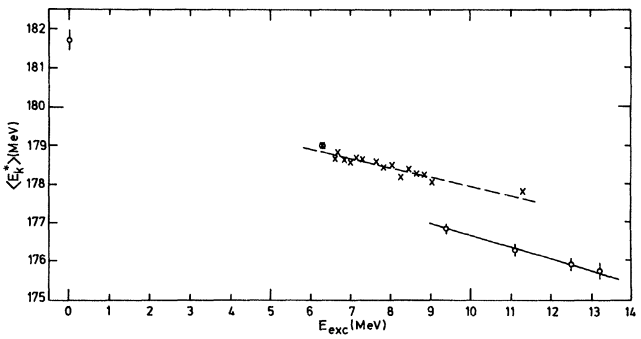

FIG. 6. $\langle E_k^* \rangle$ values as a function of the excitation energy of the compound nucleus ^{242}Pu. The data for fast-neutron-induced fission of ^{241}Pu, reported by Vorobeva *et al.* (Ref. 5), are represented by crosses. The results of this work for ^{242}Pu(sf), ^{241}Pu(n_{th},f), and ^{242}Pu(γ,f) are indicated by the circles.

different from the values for the photofission of ^{240}Pu, -0.37 ± 0.08 (Ref. 1), and ^{244}Pu, -0.40 ± 0.10 (Ref. 2). In Fig. 6 the excitation energy dependence of $\langle E_k^* \rangle$ observed for the photofission of ^{242}Pu is compared to the data for fast-neutron-induced fission of ^{241}Pu, reported by Vorobeva *et al.*[5] Compared to photofission, the value of the slope of a linear fit through the ^{241}Pu(n,f) data, -0.23 ± 0.02, is slightly smaller. More striking is the difference of about 1.5 MeV between the $\langle E_k^* \rangle$ values for photofission and neutron induced fission at the same excitation energy. In the fission of ^{240}Pu the same excitation energy dependence of $\langle E_k^* \rangle$ was observed in different reactions with low angular momentum transfer.[1] Since the photon absorption in the photon energy range considered in our experiments is predominantly $E1$ and the angular momentum transfer in neutron capture is $1-2\hbar$, Fig. 6 shows that a reaction independent behavior of $\langle E_k^* \rangle$ found for ^{240}Pu is not generally valid. This figure suggests that the behavior of the fission characteristics depends not only on the angular momentum transfer in the reaction but also on the primary reaction mechanism. This was already concluded for high angular momentum transfer reactions by Back *et al.*[23] from a study of the ^{241}Pu(^{3}He,αf) and ^{240}Pu($\alpha,\alpha' f$) reactions.

For the interpretation of the excitation energy dependence of $\langle E_k^* \rangle$ observed in our experiments, the behavior of the kinetic energy as a function of the heavy fragment mass, $\langle E_k^* \rangle(m_H^*)$, was studied for the fissioning systems considered. In Fig. 7 the $\langle E_k^* \rangle(m_H^*)$ curves for ^{242}Pu(sf), ^{241}Pu(n_{th},f), and ^{242}Pu($\gamma_{20\,MeV}$,f) are compared. The results of scission point model calculations[7] are also given in this figure. These calculations were performed by adopting a value of 0.8 MeV for the intrinsic temperature and 1 MeV for the collective temperature based on the same arguments as outlined in Ref. 6. If not indicated in Fig. 7 the uncertainties on the experimental kinetic energy values do not exceed the sizes of the points. The maximum in the experimental curves in the mass region of the closed $N=82$ neutron shell is reproduced by the calculations and can be attributed to the low average total deformation of the scission configurations for these mass splits. The systematic difference of about 20 MeV between the experimental and calculated curves is partly owing to the prescission kinetic energy contribution, which was not taken into account in the calculations.

Comparing the $\langle E_k^* \rangle(m_H^*)$ curves for ^{242}Pu(sf) and ^{241}Pu(n_{th},f), the kinetic energy is higher for spontaneous fission in the mass region 131–137, constant around mass 140, and systematically higher in thermal-neutron-induced fission for more asymmetric mass splits. This behavior is about the same as observed for ^{240}Pu. The decrease of the kinetic energy in the mass region of the spherical $N=82$ neutron shell in thermal-neutron-induced fission can be attributed in the scission point model to the diminution of the shell corrections at higher intrinsic temperatures. The constancy of the kinetic energy around mass 140, where shell effects in the fragments are of minor importance, indicates that the fission mode is strongly coupled to other degrees of freedom in the transition from the saddle to the scission point. This is in agreement with the conclusions of Nifenecker *et al.*[24] in their review paper on the dynamics of fission. The higher kinetic energies in induced fission compared to spontaneous fission for strongly asymmetric mass splits, generally observed, is difficult to explain. In scission point model calculations at different intrinsic temperatures, changes of the kinetic energy do not appear in this mass region.

The differences between the $\langle E_k^* \rangle(m_H^*)$ curves for

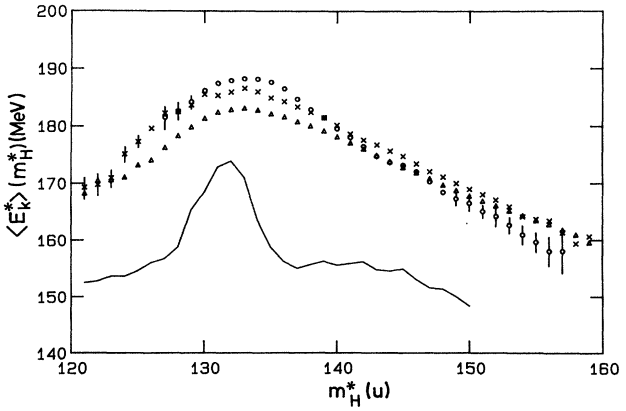

FIG. 7. Average preneutron kinetic energy as a function of the heavy fragment mass $\langle E_k^* \rangle(m_H^*)$ for ^{242}Pu(sf) (circles), ^{241}Pu(n_{th},f) (crosses), and ^{242}Pu($\gamma_{20\,MeV}$,f) (triangles). The full line represents the results of scission point model calculations (Ref. 7).

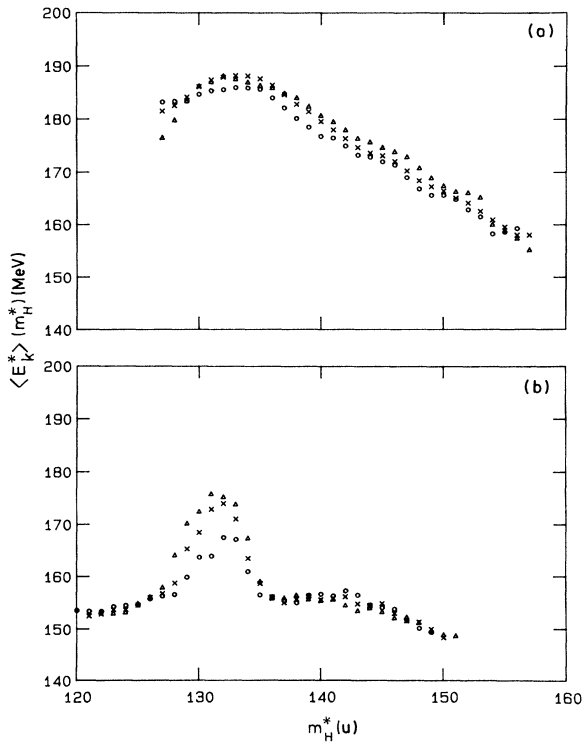

FIG. 8. A comparison of the $\langle E_k^* \rangle(m_H^*)$ behavior for the spontaneous fission of ^{240}Pu (circles), ^{242}Pu (crosses), and ^{244}Pu (triangles) obtained in our experiments is presented in (a). The results of scission point model calculations for ^{240}Pu (circles), ^{242}Pu (crosses), and ^{244}Pu (triangles) are shown in (b).

spontaneous fission and 20-MeV bremsstrahlung induced photofission of ^{242}Pu shows completely the same behavior as observed in the ^{242}Pu(sf)-^{241}Pu(n_{th},f) comparison. The stronger decrease of the kinetic energy in the spherical $N=82$ neutron shell mass region for photofission compared to thermal-neutron-induced fission is owing to the further diminution of the shell corrections at higher intrinsic temperatures.

In Fig. 8 the $\langle E_k^* \rangle (m_H^*)$ curves for the spontaneous fission of ^{240}Pu, ^{242}Pu, and ^{244}Pu, obtained in our experiments, are compared to the results of scission point model calculations for these nuclei. The higher kinetic energies for ^{242}Pu(sf) and ^{244}Pu(sf) compared to ^{240}Pu(sf) in the $N=82$ neutron shell mass region are predicted by the model and can be attributed to a higher contribution of the shell-stabilized configuration. However, the differences for more asymmetric mass splits, which are as large as in the $N=82$ neutron shell region, are not reproduced by the model. It is clear that the changes in this mass region are not owing to localized shell structures in the fragments, but are caused by systematically more compact scission shapes or/and higher prescission kinetic energies for the heavier plutonium isotopes.

The variation of the preneutron kinetic energy with the average excitation energy of the compound nucleus as a function of the heavy fragment mass $d\langle E_k^* \rangle (m_H^*)/d\langle E_{exc}(E_e) \rangle$ for the photofission of ^{242}Pu is presented in Fig. 9. The same behavior as for the photofission of ^{240}Pu (Ref. 1) and ^{244}Pu (Ref. 2) is observed. The behavior of $d\langle E_k^* \rangle (m_H^*)/d\langle E_{exc}(E_e) \rangle$ with a pronounced minimum around mass 130 shows that the systematic decrease of the average kinetic energy release in photofission is almost completely owing to the washing out of the shell structures in the fragments at higher excitation energy. The values of the slope $d\langle E_k^* \rangle (m_H^*)/d\langle E_{exc}(E_e) \rangle$ are positive in the mass region of symmetric fission although the error bars are large. Nevertheless, this positive slope was systematically observed in our earlier photofission work on ^{235}U, ^{238}U, ^{240}Pu, and ^{244}Pu.[1,2,25,26] According to Wilkins *et al.*[6] this behavior is predicted by the scission point model. The constancy of the kinetic energy for strongly asymmetric mass splits ($m_H^* > 140$), where changes in the kinetic energy caused by the diminution of the shell corrections in the potential energy of the system at higher excitation energies are not expected, indicates that the kinetic energy of the fragments is not influenced by an increase of the number of quasiparticle excitations.

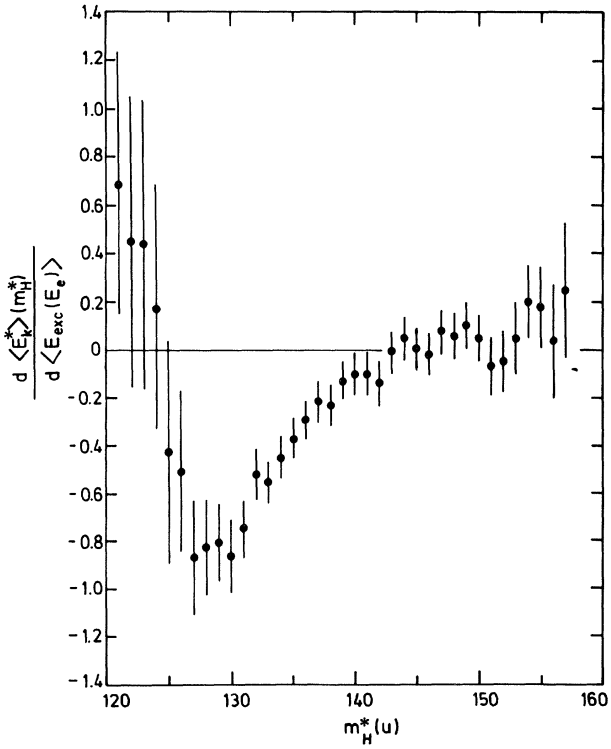

FIG. 9. Variation of $\langle E_k^* \rangle (m_H^*)$ with $\langle E_{exc}(E_e) \rangle$ for the photofission of ^{242}Pu.

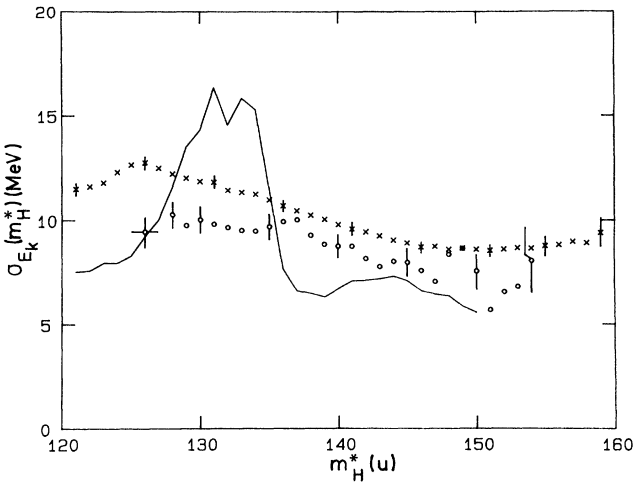

FIG. 10. Comparison of the behavior of the width of the kinetic energy distribution as a function of the heavy fragment mass $\sigma_{E_k}(m_H^*)$ for ^{242}Pu(sf) (circles) and the photofission of ^{242}Pu with 20-MeV bremsstrahlung (crosses). The results of scission point model calculations (Ref. 7) are indicated by the full line. The sizes of the error bars in the different mass regions are also given in the figure.

A direct comparison of the behavior of the width of the kinetic energy distribution as a function of the heavy fragment mass $\sigma_{E_k}(m_H^*)$ for the spontaneous and 20-MeV bremsstrahlung induced fission of ^{242}Pu is shown in Fig. 10. The same behavior as for 20-MeV bremsstrahlung induced fission was observed in the experiments performed at the other bremsstrahlung end-point energies. A pronounced maximum in the spherical $N=82$ neutron shell region as expected from the calculations is not present in the experimental curves. For spontaneous fission our results show a dip rather than a maximum in this region. This can be explained by the predominant formation of the shell-stabilized configuration. For photofission of ^{242}Pu the maximum in the $\sigma_{E_k}(m_H^*)$ curve shows up around mass 125. Owing to the use of a 40 μg/cm^2 thick electrosprayed target for the calibration with ^{241}Pu(n_{th},f), the $\sigma_{E_k}(m_H^*)$ values for this fissioning system obtained in our experiments are slightly higher than for photofission.

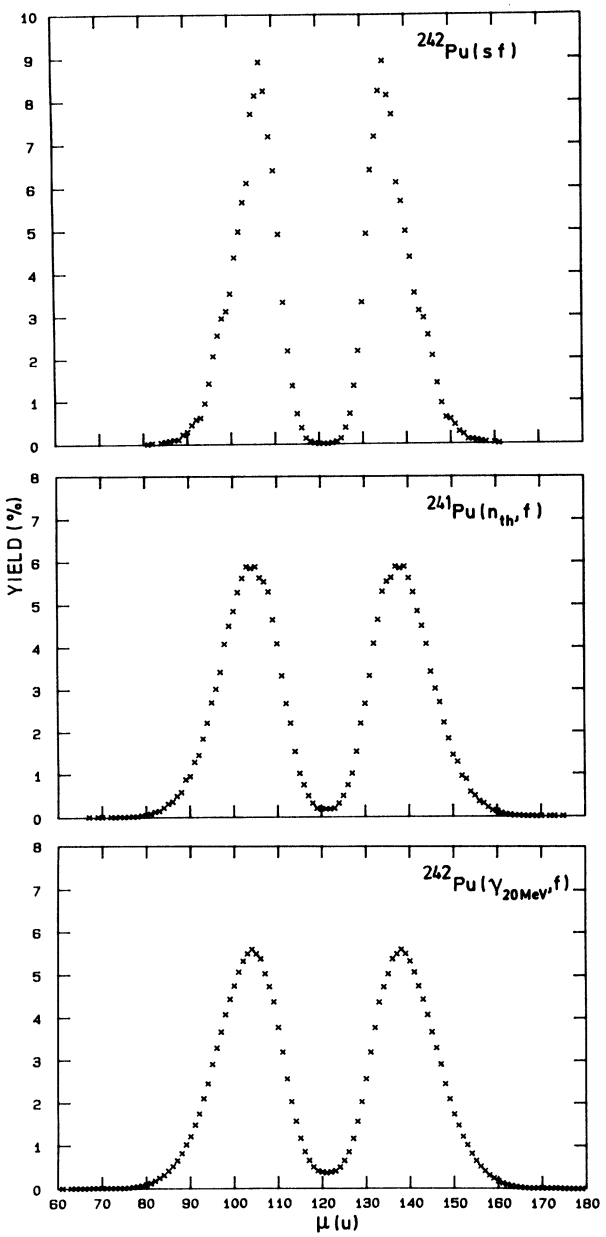

FIG. 11. Provisional mass distribution for ^{242}Pu(sf), ^{241}Pu(n_{th},f), and ^{242}Pu($\gamma_{20\,MeV}$,f).

Caïtucoli *et al.*[11] performed a detailed study of the mass and energy characteristics of the ^{241}Pu(n_{th},f) fragments using a very thin (2.3 μg/cm^2) ^{241}Pu target. According to these authors, the $\sigma_{E_k}(m_H^*)$ behavior for ^{241}Pu(n_{th},f) shows a pronounced maximum around mass 123. It is clear from Fig. 10 that this maximum is also not reproduced by the scission point model calculations. We can conclude here that the $\sigma_{E_k}(m_H^*)$ behavior cannot be understood in the scission point model.

C. Mass distribution

The provisional mass distributions for ^{242}Pu(sf), ^{241}Pu(n_{th},f), and the photofission of ^{242}Pu with 20-MeV bremsstrahlung, obtained in our experiments, are presented in Fig. 11. The mass distribution for ^{242}Pu(sf) shows a very high peak yield around mass 135 and a shoulder in the mass region 143—144. These structures are reduced drastically for ^{241}Pu(n_{th},f) and have practically disappeared for the photofission of ^{242}Pu with 20-MeV bremsstrahlung. A comparison presented in Fig. 12, of the kinetic energy distributions for the mass splits with the heavy fragment mass in the mass region 131—137, where the large differences between the mass distributions for ^{242}Pu(sf) and ^{241}Pu(n_{th},f) appear, shows that these differences are owing to high kinetic energy events. The high peak yield for ^{242}Pu(sf) can be attributed to the simultaneous occurrence of the strong spherical $N=82$ neutron shell in the heavy fragments and the deformed $N=66$ neutron shell in the light fragments. The shoulder around mass 143—144 can be explained by the influence of the deformed $N=58$ and 88 neutron shells in complementary fragments. The disappearance of the structures observed for spontaneous fission in induced fission can be understood in the scission point model by the diminution of the shell corrections at higher intrinsic temperatures.

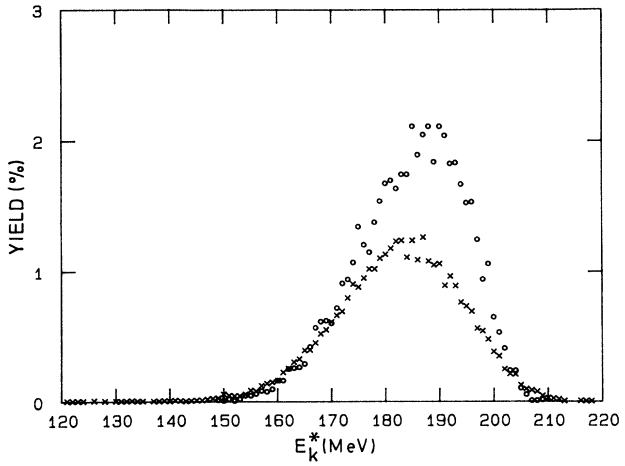

FIG. 12. Comparison of the kinetic energy distributions for the mass splits with the heavy fragment in the mass region 131—137 for ^{242}Pu(sf) (circles) and ^{241}Pu(n_{th},f) (crosses). In the normalizations used in this figure a yield of 100% corresponds to the total number of fission events.

The main characteristics of the overall mass distributions for the fissioning systems studied are also summarized in Table I. As generally observed, the peak-to-valley ratio P/V decreases with increasing excitation energy. The P/V value for ^{241}Pu(n_{th},f), obtained in our experiments, is too low and has no sense as we used a relatively thick electrosprayed ^{241}Pu target. Caïtucoli *et al.*[11] reported a value 265±16 for the asymmetric-to-symmetric fission ratio for ^{241}Pu(n_{th},f).

The values of the average preneutron mass of the light and heavy fragment peak $\langle m_L^* \rangle$ and $\langle m_H^* \rangle$ for ^{242}Pu(sf) and ^{241}Pu(n_{th},f) obtained in this work and given in Table I are in very good agreement with the results of Dyachenko *et al.*[3] and Allaert *et al.*[4] Dyachenko *et al.*[3] reported for the $\langle m_L^* \rangle$ and $\langle m_H^* \rangle$ values in ^{242}Pu(sf) 104.43±0.06 and 137.57±0.06, respectively, while Allaert *et al.*[4] reported

104.50±0.05 and 137.50±0.05, respectively. The corresponding values for ^{241}Pu(n_{th},f) are 102.52±0.02, 139.48±0.02 following Dyachenko *et al.*,[3] and 102.45±0.04, 139.55±0.04, according to Allaert *et al.*[4]

From Table I it is clear that the average light and heavy fragment masses of the provisional mass distribution $\langle \mu_L \rangle$ and $\langle \mu_H \rangle$ as well as the same parameters of the preneutron mass distribution $\langle m_L^* \rangle$ and $\langle m_H^* \rangle$ for ^{241}Pu(n_{th},f) are shifted over two mass units towards asymmetric fission compared to ^{242}Pu(sf). A similar shift over one mass unit was also observed in our comparative study of ^{240}Pu(sf) and ^{239}Pu(n_{th},f). These changes are mainly owing to the decrease of the influence of the spherical $N=82$ neutron shell in induced fission. Unik *et al.*[23] also performed a systematic study of the $\langle m_L^* \rangle$ and $\langle m_H^* \rangle$ values for spontaneous and thermal-neutron-induced fissioning systems. The data reported by these authors together with the results of our studies for the plutonium isotopes are shown in Fig. 13. For ^{242}Pu(sf) and ^{244}Pu(sf) the experimental values differ from the systematics by 2.5 mass units. For ^{240}Pu(sf) the difference is only one mass unit. These differences from the systematics are caused predominately by the strong influence of the spherical $N=82$ neutron shell in the spontaneous fission of the plutonium isotopes.

Table I shows that $\langle m_L^* \rangle$ and $\langle m_H^* \rangle$ for photofission of ^{242}Pu are independent of the bremsstrahlung end-point energy. However, compared to ^{241}Pu(n_{th},f), the values of the average light and heavy fragment masses for the photofission of ^{242}Pu are shifted 0.5 mass units towards asymmetric fission. A difference between the $\langle m_L^* \rangle$ and $\langle m_H^* \rangle$ values for photofission and thermal neutron induced fission was not observed for ^{240}Pu. As already mentioned, a systematic difference exists also between the $\langle E_k^* \rangle$ values for neutron induced fission of ^{241}Pu and photofission of ^{242}Pu, where the corresponding values for ^{240}Pu are the same taking into account the given uncertainties.

The dispersion on the mass distribution σ_μ for ^{242}Pu(sf), obtained in our work, 5.27±0.08, is significantly lower than the corresponding values, reported by Allaert *et al.*,[4] 5.82, and by Dyachenko *et al.*,[3] 5.63. This difference illustrates the better resolution in our experiments, caused predominantly by the use of a ^{242}Pu target prepared by the evaporation technique. In their experiments Allaert *et al.*[4] and Dyachenko *et al.*[3] used electrosprayed targets. As also observed in our studies of the fission of ^{240}Pu and ^{244}Pu, σ_μ is increased in induced fission compared to spontaneous fission. The systematic increase of σ_μ with the bremsstrahlung end-point energy, observed in the photofission of ^{242}Pu, is caused by the increase of the symmetric fission yield.

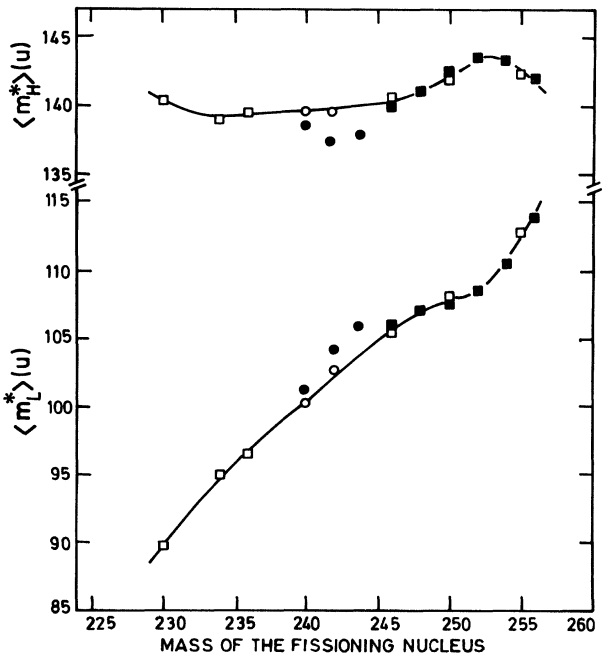

FIG. 13. Comparison of the $\langle m_L^* \rangle$ and $\langle m_H^* \rangle$ values for the spontaneous fission and thermal-neutron-induced fission of the plutonium isotopes, obtained in our work and represented by the closed and open circles, respectively, with the systematics of Unik *et al.* (Ref. 22). The data for spontaneous and thermal-neutron-induced fission, reported by Unik *et al.* (Ref. 22), are indicated by the closed and open squares.

IV. CONCLUSIONS

The value for the neutron emission width to fission width ratio Γ_n/Γ_f for ^{242}Pu, deduced in this work from the measured photofission yields, together with previous results on ^{242}Pu and ^{244}Pu, are in agreement with an exponential increase of Γ_n/Γ_f with the difference $E_f - B_n$ between the fission barrier height and the neutron binding energy.

The overall total kinetic distribution for ^{242}Pu(sf) is strongly asymmetric, while the overall mass distribution has a very high peak yield (9%) around mass 135. Furthermore, the experimental $\langle E_k^* \rangle$ value for ^{242}Pu(sf), 181.69±0.24 MeV, is 4.4 MeV higher than the expectation value following the systematics of Unik *et al.*[22] Compared to these systematics, the average light and heavy fragment masses $\langle m_L^* \rangle$ and $\langle m_H^* \rangle$ for this fissioning system are shifted over 2.5 mass units towards symmetry. These effects can be understood in the scission point model[6,7] by the strong preferential formation of a shell-stabilized scission configuration with neutron number of the heavy fragment in the vicinity of the spherical $N=82$ neutron shell and neutron number of the light fragment in the vicinity of the deformed $N=66$ neutron shell. The structures in the overall distributions and the deviations from the systematics are seriously reduced in ^{241}Pu(n_{th},f) and have practically disappeared in the photofission of ^{242}Pu owing to the diminution of the shell corrections in the potential energy of the system at higher intrinsic temperatures.

In the photofission of ^{242}Pu, $\langle E_k^* \rangle$ is decreasing for increasing compound nucleus excitation energy $\langle E_{exc}(E_e) \rangle$ with a value -0.30 ± 0.04 for the slope $d\langle E_k^* \rangle / d\langle E_{exc}(E_e) \rangle$. In the excitation energy range, where the results for photofission and fast-neutron-induced fission can be compared, the $\langle E_k^* \rangle$ values for neutron induced fission are systematically about 1.5 MeV higher. This would indicate that the behavior of the fis-

sion characteristics depends also on the primary reaction mechanism.

An investigation of the energy-mass correlations shows that the decrease of $\langle E_k^* \rangle$ with the excitation energy in photofission is almost completely owing to the diminution of the shell corrections in the spherical $N=82$ shell mass region. From a direct comparison of the $\langle E_k^* \rangle(m_H^*)$ curves for ^{242}Pu(sf) and ^{241}Pu(n_{th},f) in the vicinity of mass 140, we can conclude that the fission mode is strongly coupled to other degrees of freedom in the transition from the saddle to the scission point, in agreement with Nifenecker *et al.*[24]

The higher kinetic energies for ^{242}Pu(sf) and ^{244}Pu(sf) compared to ^{240}Pu(sf) for the mass splits with the heavy fragment in the $N=82$ neutron shell mass region are reproduced by the scission point model calculations.[7] However, the differences observed between the $\langle E_k^* \rangle(m_H^*)$ curves for ^{240}Pu(sf), ^{242}Pu(sf), and ^{244}Pu(sf) for strongly asymmetric mass splits ($m_H^* > 140$) are not expected by the scission point model. A prominent maximum in $\sigma_{E_k}(m_H^*)$ in the $N=82$ neutron shell mass region, predicted by this model, is also not present in the experimental curves for ^{242}Pu(sf), ^{241}Pu(n_{th},f), and ^{242}Pu(γ,f). A comparison of the experimentally determined behavior of the fission characteristics and the results of scission point model calculations[7] shows that although some gross features of the mass and kinetic energy distributions are reproduced by this model, quantitatively serious discrepancies still exist.

ACKNOWLEDGMENTS

This research was supported by the Interuniversity Institute for Nuclear Science-National Fund for Scientific Research. Dr. A. J. Deruytter is acknowledged for his continuous interest. Thanks are expressed to the linac team of our laboratory for the operation of the accelerator and to Dr. R. Van de Vyver and Dr. E. Kerkhove for their aid during the cross section measurements. Thanks are also due to J. Moreau and Dr. K. Heyde for performing the scission point model calculations. Finally, the authors are indebted to Dr. M. Nève de Mévergnies, Dr. C. Wagemans, and Dr. E. Allaert for their help during the measurements at the SCK-CEN, Mol, Belgium.

[1]H. Thierens, A. De Clercq, E. Jacobs, D. De Frenne, P. D'hondt, P. De Gelder, and A. J. Deruytter, Phys. Rev. C 23, 2104 (1981).

[2]H. Thierens, A. De Clercq, E. Jacobs, M. Piessens, P. D'hondt, and D. De Frenne, Phys. Rev. C 27, 1117 (1983).

[3]N. Dyachenko, V. Kabenin, N. Kolosov, B. Kuzminov, and A. Sergachev, Yad. Fiz. 17, 696 (1973) [Sov. J. Nucl. Phys. 17, 362 (1973)].

[4]E. Allaert, C. Wagemans, G. Wegener-Penning, A. J. Deruytter, and R. Barthelemy, Nucl. Phys. A380, 61 (1982).

[5]V. Vorobeva, B. Kuzminov, and V. Manokhin, International Atomic Energy Agency Report INDC (CCP) 128G (1979).

[6]B. D. Wilkins, E. P. Steinberg, and R. R. Chasman, Phys. Rev. C 14, 1832 (1976).

[7]J. Moreau, K. Heyde, and M. Waroquier, Phys. Rev. C 28, 1640 (1983).

[8]H. Scmitt, W. Gibson, J. Neiler, F. Walter, and T. Thomson, in *Proceedings of the Second International Atomic Energy Agency Symposium on Physics and Chemistry of Fission, Vienna, 1965* (IAEA, Vienna, 1965), Vol. I, p. 531.

[9]J. Neiler, F. Walter, and H. Schmitt, Phys. Rev. 149, 894 (1966).

[10]H. Schmitt, J. Neiler, and F. Walter, Phys. Rev. 141, 1146 (1966).

[11]F. Caïtucoli, C. Wagemans, P. Perrin, E. Allaert, P. D'hondt, and M. Asghar, Nucl. Phys. A369, 15 (1981).

[12]J. Boldeman, J. Nucl. Energy 22, 63 (1968).

[13]H. Condé, J. Hansen, and M. Holmberg, J. Nucl. Energy 22, 53 (1968).

[14]N. S. Rabotnov, G. N. Smirenkin, A. S. Soldatov, L. N. Usachev, S. P. Kapitza, and Yu. M. Tsipenyuk, Yad. Fiz. 11, 508 (1970) [Sov. J. Nucl. Phys. 11, 285 (1970)].

[15]D. M. Crawford, R. Koch, and H. H. Thies, Nucl. Instrum. Methods 109, 573 (1973).

[16]J. T. Caldwell, E. J. Dowdy, B. L. Berman, R. A. Alvarez, and P. Meyer, Phys. Rev. C 21, 1215 (1980).

[17]J. D. Cramer and H. C. Britt, Nucl. Sci. Eng. 41, 177 (1970).

[18]R. Vandenbosch and J. R. Huizenga, *Nuclear Fission* (Academic, New York, 1973).

[19]H. C. Britt, in *Proceedings of the Fourth International Atomic Energy Agency Symposium on Physics and Chemistry of Fission, Jülich, 1979* (IAEA, Vienna, 1980), Vol. I, p. 3.

[20]A. H. Wapstra and K. Bos, At. Data Nucl. Data Tables 19, 215 (1977).

[21]L. J. Schiff, Phys. Rev. 83, 252 (1951).

[22]J. P. Unik, J. E. Gindler, L. E. Glendenin, K. J. Flynn, A. Gorski, and R. K. Sjoblom, in *Proceedings of the Third International Atomic Energy Agency Symposium on Physics and Chemistry of Fission, Rochester, 1973* (IAEA, Vienna, 1974), Vol. II, p. 19.

[23]B. B. Back, J. M. Lebowitz, and K. L. Wolf, Phys. Rev. C 20, 1819 (1979).

[24]H. A. Nifenecker, J. Blachot, J. P. Bocquet, R. Brissot, J. Crançon, C. Hamelin, G. Mariolopoulos, and C. Ristori, in *Proceedings of the Fourth International Atomic Energy Agency Symposium on Physics and Chemistry of Fission, Jülich, 1979* (IAEA, Vienna, 1980), Vol. II, p. 35.

[25]E. Jacobs, A. De Clercq, H. Thierens, D. De Frenne, P. D'hondt, P. De Gelder, and A. J. Deruytter, Phys. Rev. C 20, 2249 (1979).

[26]E. Jacobs, A. De Clercq, H. Thierens, D. De Frenne, P. D'hondt, P. De Gelder, and A. J. Deruytter, Phys. Rev. C 24, 1795 (1981).